

Crystal chemistry of zemannite-type structures: I. A re-examination of zemannite from Moctezuma, Mexico

OWEN P. MISSEN^{1,2,a}, STUART J. MILLS¹, JOHN SPRATT³, WILLIAM D. BIRCH¹ and JOËL BRUGGER⁴

¹Geosciences, Museums Victoria, GPO Box 666, Melbourne VIC 3001, Australia

*Corresponding author, e-mail: omissen@museum.vic.gov.au

²School of Chemistry, University of Melbourne, Melbourne VIC 3010, Victoria, Australia

³Department of Core Research Laboratories, Natural History Museum, Cromwell Road, London SW7 5BD, England

⁴School of Earth, Atmosphere and the Environment, Monash University, Clayton VIC 3800, Australia

^aNow also at School of Earth, Atmosphere and Environment, Monash University, Clayton VIC 3800, Australia.

Abstract: The crystal structure of zemannite has been re-examined in order to address several features worthy of discussion. Analyses were performed on the type specimen and on material representative of Moctezuma. Type zemannite was found to refine in the space group $P6_3$ with $a = 9.3877(5)$, $c = 7.6272(4)$ Å and $V = 582.12(7)$ Å³, whilst the unit-cell parameters in the same space group for the material representative of Moctezuma were $a = 9.3921(13)$, $c = 7.6230(15)$ Å and $V = 582.3(2)$ Å³. The structural refinements undertaken were able to confirm for the first time the presence of a hydrogen bonding network in zemannite. An examination of the refinement of type zemannite in $P6_3/m$ was also undertaken, showing that refining in the higher-symmetry space group does not show the ordering of framework octahedral metal cations. Zemannite-type minerals should therefore be refined in a non-centrosymmetric space group if possible, allowing the occupancies of the framework metal cations to refine. The chemical composition of zemannite was analysed by EMPA and by ICP-AES, showing conclusively that zemannite contains negligible Na, though the presence of Na should always be checked when analysing zemannite-type minerals. We also recommend that the formula of zemannite is revised to $Mg_{0.5}ZnFe^{3+}(Te^{4+}O_3)_3 \cdot (3+n)H_2O$, where $0 \leq n \leq 1.5$ from the current definition of $Mg_{0.5}ZnFe^{3+}(Te^{4+}O_3)_3 \cdot 4.5H_2O$ to better reflect the variable degree of hydration, since the type specimen is almost fully dehydrated and only contains three H₂O molecules per formula unit.

Key-words: zemannite; zeolitic; crystal structure; Moctezuma; space group; substitution; tellurate.

1. Introduction

Zemannite, first recorded in 1961, was one of the first tellurium oxysalts discovered at Moctezuma mine, Sonora, Mexico (29°48'N, 109°40'W), and remains one of the most common minerals found there (Mandarino & Williams, 1961). Zemannite and the isostructural minerals kinichilite, keystoneite, and ilirneyite all have a zemannite-type structure. Aside from zemannite itself, none of these minerals has a published crystal structure (Christy *et al.*, 2016).

When first published in 1961, the chemical description of zemannite was incorrect, listing only essential zinc and tellurium (Mandarino & Williams, 1961). Matzat (1967) reported the structure as $\{(Zn,Fe)_2[TeO_3]_3\}Na_xH_{2-x}yH_2O$. This formula shows uncertainties around the Zn:Fe³⁺ ratio, suggested that Fe was ferrous and misidentified the channel species as Na⁺ and H⁺. Miletich (1995a) later concluded that sodium had a negligible presence in natural zemannite and kinichilite (the Mn²⁺ analogue of zemannite), based on EMPA analysis on samples from the type localities of these two minerals. He also concluded that hydrated magnesium

octahedra half-occupy the channel sites. However, this study failed to determine the chemistry of material from type zemannite, meaning that the identity of the cations within the hexagonal channels of the mineral is still contentious.

The hexagonal framework structure of zemannite has been known for 50 years (Fig. 1), and is formed from M_2O_9 dimers and tellurite pyramids, with channels extending infinitely in the c direction (Matzat, 1967). More generally, the zemannite structure is a $[M_2^{n+}(Te^{4+}O_3)_3]^{2n-6}$ framework, where M^{n+} represents one or more octahedral cations. All known naturally occurring zemannite compositions cluster around an ideal 1:1 ratio of $M^{2+}:M^{3+}$ metal cations (Miletich, 1995a). Zemannite-type minerals are defined as having 4.5 water molecules per formula unit (*pfu*) (Pasero, 2018), though more recently have been reported to contain 3.9 H₂O molecules *pfu* (Cametti *et al.*, 2017). Despite this well-defined framework, it is not conclusively known how Zn and Fe³⁺ occupy the framework octahedral metal sites (*i.e.*, whether they are in an ordered or disordered configuration). Most recently, an ordered configuration was postulated by Cametti *et al.* (2017), without

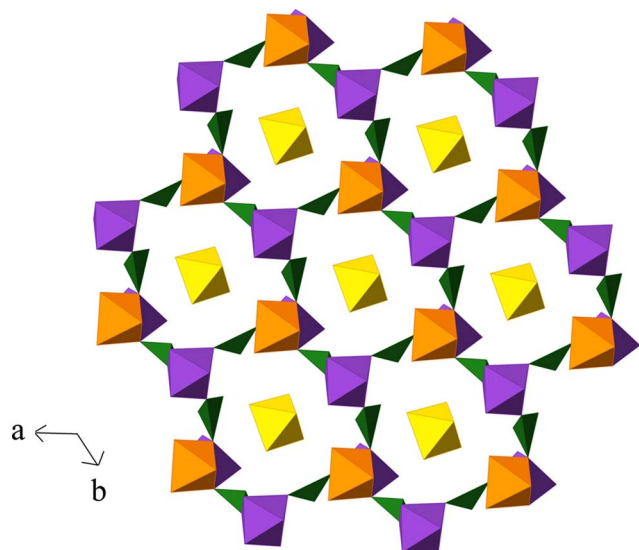


Fig. 1. A cross-section of ideal zemannite with a $\text{Fe}^{3+}:\text{Zn}$ ratio of 1:1. The hexagonal channels extend infinitely into the page in the c direction but only a thin section is shown for clarity. Framework Te^{4+}O_3 pyramids are shown in dark green, Fe^{3+}O_6 dominant octahedra in purple and ZnO_6 dominant octahedra in orange. Yellow MgO_6 octahedra are found in the channels. H atoms on channel oxygens are omitted for clarity.

allowing the bond lengths of the two framework cation sites to refine separately.

2. Natural zemannite specimen descriptions

Two natural zemannite specimens were analysed in this study. One was the type zemannite specimen, from the Royal Ontario Museum, Toronto, Canada, specimen number M25933, which is hereafter referred to as zemtype. The type specimen is from the Moctezuma mine, Sonora, Mexico ($29^{\circ}48'\text{N}$, $109^{\circ}40'\text{W}$). The components of this specimen used for analysis consist of several grains of zemannite embedded in resin, which were used for EMPA analysis, and a single crystal of zemannite glued onto a glass fibre, used for room-temperature single-crystal analysis (Fig. 2).

The second natural zemannite is representative of material from Moctezuma, used for comparison with the type material. This zemannite specimen was one of the highest quality amongst more than ten zemannite-bearing specimens collected by one of the authors (JB) from the dumps of the Moctezuma mine in 2004. The specimen contains numerous elongated red-brown transparent crystals on the surface of a rock otherwise rich in quartz, calcite, and tellurite (Fig. 3). This zemannite specimen, hereafter referred to as zemmoc, is registered in the collections of Museums Victoria, registration number M53996.

3. Description and comparison of zemannite chemistry

The analysis of the chemistry of zemtype and zemmoc was performed using two methods to double check for the



Fig. 2. The type zemannite (zemtype) single crystal, viewed from above. Note the highly defined crystal facets. The long axis of the crystal (top left to bottom right) is 0.223 mm long (M25933, Royal Ontario Museum).

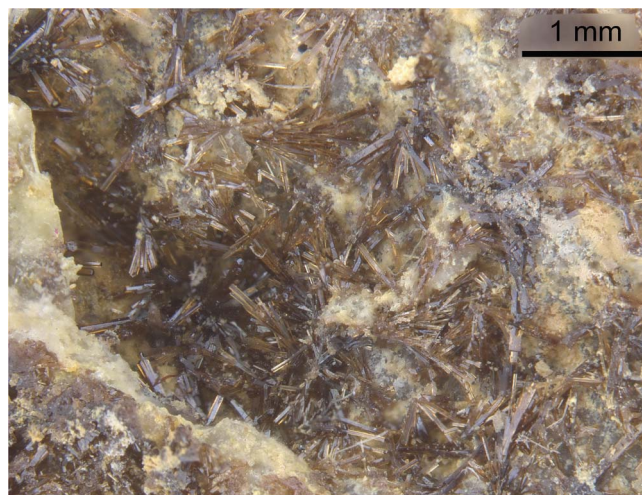


Fig. 3. A large number of brown, elongated crystals of zemannite on the zemmoc specimen (M53996, Museums Victoria).

presence of sodium in zemannite. The conventional method of EMPA was initially used. However, peak overlap of Na and Zn is a common problematic interference in EMPA analyses, and Na detection limits are considerably higher in EMPA than in Inductively Coupled Plasma Atomic Emission Spectroscopy (ICP-AES). Whilst the EMPA experiments on both zemannites showed negligible (<0.12 wt%) Na, to double check this result zemmoc was also analysed by ICP-AES. The initial reporting of sodium in zemannite (Matzat, 1967) means that it is especially important that this analysis is accurate.

3.1. EMPA of zemtype and zemmoc

Quantitative chemical analyses of both zemannite specimens were performed on a Cameca SX100 Electron Microprobe (WDS mode, 20 kV, 20 nA, 5 μm beam diameter and

Table 1. Chemical composition data for zemtype and zemmoc Na₂O was negligible in all analyses (both in EMPA and in ICP-AES). All metallic-character elements were analysed by ICP-AES except for Te. A total wt% is not given for this reason. In ICP-AES, the wavelengths of measurement (nm) were 589.592 (Na), 280.271 (Mg), 257.610 (Mn), 238.204 (Fe) and 206.200 (Zn).

Oxide	Zemtype EMPA (5 analyses)			Zemmoc EMPA (22 analyses)			Zemmoc ICP-AES	
	Average	Range	St dev	Average	Range	St dev	Average	St dev
Na ₂ O	<0.12			<0.12			<5 × 10 ⁻⁶	
MgO	2.56	2.33–2.69	0.14	2.82	2.60–3.09	0.14	2.36	0.02
Mn ₂ O ₃	0.45	0.24–0.66	0.18	0.67	0.29–2.83	0.56	0.57	0.00
Fe ₂ O ₃	12.7	11.6–14.3	0.99	12.0	10.6–12.9	0.64	11.92	0.14
ZnO	10.4	8.7–11.5	1.04	12.8	12.0–14.5	0.63	10.22	0.15
TeO ₂	68.9	68.6–69.2	0.25	67.8	67.3–68.5	0.39	NA	NA
H ₂ O*	8.03	8.00–8.07	0.03	9.08	8.97–9.22	0.05	NA	NA
Total	103.10			105.27			NA	

*Calculated based on 3.06 H₂O *pfu* for zemtype and 3.42 H₂O *pfu* for zemmoc, based on site refining of the channel sites.

PAP matrix correction) at the Imaging and Analysis Centre, Core Research Laboratories, Natural History Museum, London. The standards used were: jadeite (Na), synthetic forsterite (Mg), wollastonite (Ca), manganese titanium oxide (Mn), haematite (Fe), sphalerite (Zn) and TeO₂ (Te). Results are recorded to one decimal place for Fe, Zn and Te as relatively low values of voltage and current were used to reduce expected dehydration during analysis. Analytical results are shown in Table 1.

Both specimens yielded compositions containing essential Mg, Fe, Zn and Te. Minor Mn (<3 wt%, generally <1 wt%) was present in both specimens. Ca was detected in zemtype and Co and Cu in zemmoc, all with an average level ≤0.05 wt%. Na levels were below the detection limit of 0.12 wt% Na, and no other elements were detected using EMPA. H₂O was calculated based on an ideal 5.5 total cations (0.5 Mg + 1 Zn + 1 Fe + 3 Te) and 9 total anions (9 O) *pfu*, determined by the crystal structure analysis (see below). The substituting Mn was treated as Mn³⁺ based on anomalous grains in zemmoc. Based on the crystal structure, water was calculated as 3.06 H₂O molecules *pfu* for zemtype and 3.42 H₂O molecules *pfu* for zemmoc. The empirical formula (based on 9 O anions *pfu*) for zemtype is Mg_{0.44}Mn_{0.04}Fe_{1.10}Zn_{0.89}Te_{2.98}H_{6.12}O_{12.06}. For zemmoc, the empirical formula is Mg_{0.48}Mn_{0.06}Fe_{1.03}Zn_{1.08}Te_{2.91}H_{6.84}O_{12.42}. Zemtype and zemmoc are thus both ideally Mg_{0.5}Fe³⁺ZnTe⁴⁺₃H₆O₁₂, when Fe³⁺:Zn is exactly 1:1. The standardised ideal formula for these minerals is Mg_{0.5}ZnFe³⁺(Te⁴⁺O₃)₃·3H₂O, which requires MgO 2.82%, ZnO 11.37%, Fe₂O₃ 11.37%, TeO₂ 66.90% and H₂O 7.55%, total 100 wt%.

3.2. ICP-AES of zemmoc

A 0.50 mg sample of zemannite crystals was selected from the zemmoc (M53996) specimen and digested in *aqua regia* (1 mL, 3 parts HCl to 1 part HNO₃) at 80 °C for 2 h, then diluted to 10 mL with deionised water and left to cool overnight.

The analysis was performed on a PerkinElmer Optima 4300 DV Optical Emission Spectrometer (TrACEES platform, School of Chemistry, University of Melbourne). Calibration was performed with 0.1, 1, 5, 10 and 20 mg/L

solutions of Na, Mg, Mn, Fe and Zn cations with suitable soluble counter-anions (ICP-AES is not valence sensitive). A small amount of the diluted zemmoc sample was aspirated into the flame and analysed five times in quick succession, with detection at standard wavelengths of emission of each metal. Analytical results are summarised in Table 1. Na was below ICP-AES detection limits (*i.e.* no more than 0.05 ppm Na, better expressed as no more than 0.05 µg Na per gram of zemannite). By first averaging the results recorded from each of the three wavelengths, the formula of the cationic components of zemmoc is Mg_{0.42}Mn_{0.05}Fe_{1.07}Zn_{0.90} from ICP-AES (based on a total charge of +6 and treating Mn as trivalent). This result is comparable to the result obtained with EMPA, with both techniques showing a slight Fe dominance over Zn.

3.3. Comparison and discussion of zemannite chemical composition

The analyses confirm that type zemannite contains essential Mg, Zn, Fe³⁺ and Te⁴⁺. EMPA and ICP-AES data in conjunction strongly suggest that no Na is present in either zemannite. Mg levels in both zemannites are slightly lower than 0.5 atoms *pfu* to allow for charge balance since the level of ferric iron is slightly greater than the amount of zinc. Manganese is present in both samples, showing that there is usually partial substitution towards the Mn analogues of zemannite. Depending on the manganese valence in individual grains, Mn²⁺ could be substituting for Zn²⁺, or Mn³⁺ for Fe³⁺. Our results show that it is more likely that Mn³⁺ is present in zemannite, based on the analysis of one anomalously zemmoc grain. An anomalously high Mn wt% occurred concurrently with a decrease in the Fe³⁺ wt% (Mn:Fe ratio of 1.63), indicating that the substitution occurring in zemmoc is most likely to be Mn³⁺ for Fe³⁺, although this may not be the case for all of the zemannite grains analysed. This substitution corresponds to an Fe-rich form of the zemannite-type mineral ilirneyite (the Mn³⁺ analogue of zemannite, in this case Mn_{0.61}Fe_{0.39} in the trivalent cation site), and shows that substitution can occur readily in zemannite depending on the local environment. Due to the distorting effect this analysis would otherwise have had on

Table 2. Crystallographic information relating to data collection and refinement of the two zemannites: zemtype and zemmoc.

	Zemtype	Zemmoc
Crystal data		
Ideal chemical formula	Mg _{0.51} Fe _{1.02} Zn _{0.98} (Te ⁴⁺ O ₃) ₃ ·3.06H ₂ O	Mg _{0.56} Fe _{0.91} Zn _{1.09} (Te ⁴⁺ O ₃) ₃ ·3.36H ₂ O
Crystal system, Space group	Hexagonal, <i>P</i> 6 ₃	Hexagonal, <i>P</i> 6 ₃
Temperature (K)	293(2)	100(2)
<i>a</i> , <i>c</i> (Å)	9.3877(5), 7.6272(4)	9.3921(13), 7.6230(15)
<i>V</i> (Å ³)	582.12(7)	582.3(2)
<i>Z</i>	2	2
<i>D</i> _x calc (g cm ⁻³)	4.043	4.124
Radiation type and wavelength (Å)	MoKα, λ = 0.71073	Synchrotron, λ = 0.71073
μ (mm ⁻¹)	10.726	10.828
Crystal dimensions (mm)	0.085 × 0.089 × 0.223	0.006 × 0.007 × 0.013
Reflections for cell refinement, <i>I</i> > 4σ(<i>I</i>)	1153	388
Data collection		
Crystal description	Hexagonal prismatic, light orange rod	Hexagonal prismatic, light brown rod
Diffractometer	SuperNova (CCD detector)	Dectris EigerX 16M
θ (°) range	3.663, 36.205	2.504, 32.203
Indices range of <i>h</i> , <i>k</i> , <i>l</i>	<i>h</i> : -15 to 10, <i>k</i> : -14 to 15, <i>l</i> : -12 to 9	<i>h</i> : ±12, <i>k</i> : ±12, <i>l</i> : ±8
Absorption correction	Multi-scan (SADABS, Bruker, 2001)	Multi-scan (SADABS, Bruker, 2001)
<i>T</i> _{max} , <i>T</i> _{min}	0.47731, 1	0.3344, 0.4345
No. of measured, independent and observed [<i>I</i> > 2σ(<i>I</i>)] reflections	2934, 1494, 1248	10791, 1061, 1058
<i>R</i> _{int}	0.0343	0.0582
Data completeness to 25.242°θ (%)	99.7	95.3
Refinement		
Number of reflections, parameters, restraints	1494, 57, 1	1061, 69, 5
<i>R</i> ₁ [<i>F</i> ² > 2σ(<i>F</i> ²)], <i>R</i> ₁ (all)	0.0346, 0.0449	0.0254, 0.0255
<i>wR</i> ₂ [<i>F</i> ² > 2σ(<i>F</i> ²)], <i>wR</i> ₂ (all)	0.0742, 0.0803	0.0704, 0.0704
<i>GoF</i> (<i>F</i> ²)	1.026	1.237
Δρ _{max} , Δρ _{min} (e Å ⁻³)	-1.70, 2.19	-1.81, 2.78

the Mn contents of zemmoc, it was excluded from the EMPA calculations.

Despite observed variation away from a 1:1 ratio of Zn and Fe³⁺ in some EMPA analyses, an ideal zemannite will still contain two framework transition metal cations *pfu*. Variation of 10% away from 1:1 is common and expected for natural zemannites (Miletich, 1995a), but variation to levels significantly beyond 10% has only been commonly observed in synthetic zemannites.

4. Comparison of zemannite crystal structures

4.1. Single-crystal diffraction of zemtype

Single-crystal X-ray diffraction of zemtype was carried out on a SuperNova diffractometer (by Rigaku Oxford Diffraction) at the School of Chemistry, University of Melbourne, Australia. The zemtype crystal was analysed by inserting the glass fibre with the 85 × 89 × 223 μm type crystal (Fig. 1) attached into a goniometer. Data were collected at 293 K by a CCD detector and Mo Kα radiation. Full details of data collection and structure refinement are provided in Table 2.

A full sphere of reflection data was collected to θ = 36.205° with 99.7% completeness to θ = 25.242°. Reflection intensities were integrated, corrected for Lorentz and polarisation effects and converted to structure factors using the program CrysAlisPro[®] (Rigaku Oxford Diffraction). Systematic absences were most consistent with 6/*m* symmetry. Reflec-

tion merging in Laue class, not group 6/*m* gave an *R*_{int} value of 0.0343. Consequently, the full dataset to θ = 36.205° was used without truncation.

Structure solution was carried out by direct methods using SHELXS (Sheldrick, 2008) and structure refinement by full-matrix least-squares was implemented by SHELXL (Sheldrick, 2015). All atom positions, anisotropic displacement parameters (*U*_{ij}) and the occupancies of the channel sites (see Table 2) were refined with reflection weighting and converged to final *R*₁ and *wR*₂ values of 0.0346 and 0.0746, respectively.

4.2. Single-crystal diffraction of zemmoc

Single-crystal X-ray diffraction on zemmoc was carried out on the micro-focus macromolecular beam line MX2 at the Australian Synchrotron, part of ANSTO. A 6 × 7 × 13 μm pale-brown single crystal of zemannite was selected from specimen M53996. Data were collected at 100 K by a Dectris EigerX 16 M detector and monochromatic radiation with a wavelength of 0.71073 Å. Full details of data collection and structure refinement are provided in Table 2.

After processing the data using XDS (Kabsch, 2010), XPREP (Bruker, 2001) and SADABS (Bruker, 2001), 10791 reflections were found with an *R*_{int} of 0.0582. Structure solution was carried out by direct methods using SHELXS (Sheldrick, 2008). Structure refinement by full-matrix least-squares was implemented by SHELXL (Sheldrick,

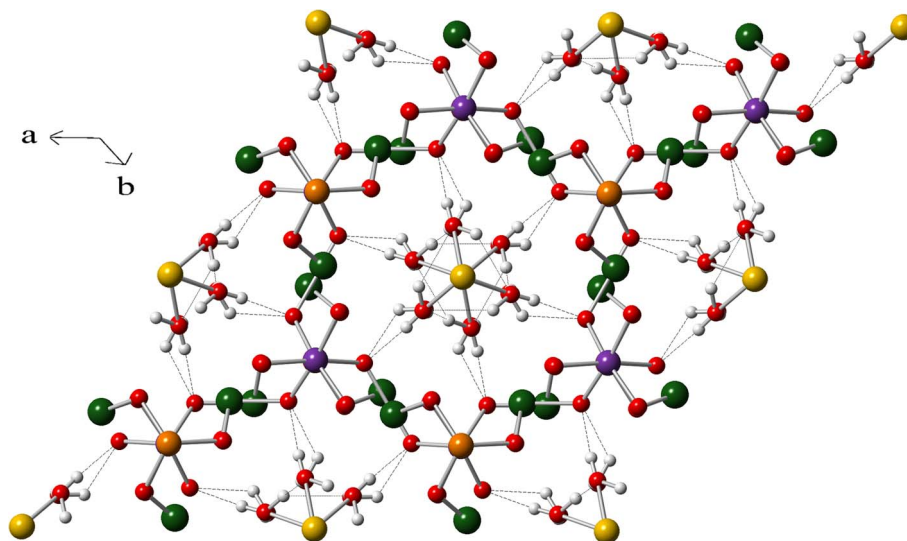


Fig. 4. The hydrogen bonding network in zemannite, as determined in zemmoc. Two H-bonds are formed to the framework atom O1, while another two are formed as cross-links within the channel water molecules.

2015), showing one Te site, two framework octahedral sites, one channel octahedral metal site and five oxygen atom sites. All atom positions and anisotropic displacement parameters (U_{ij}) were refined (see Table 2) and converged to final R_1 and wR_2 values of 0.0254 and 0.0704 respectively.

4.3. Refinement discussion for zemtype and zemmoc

Both of the zemannite crystals were shown by the crystal structure refinement to be twinned, therefore a twin scale factor was refined for each. Both twin scale factors were very close to 0.5.

The two framework octahedral metal sites were both refined with Fe and Zn on each site. The occupancies of the metals were fixed at a ratio determined by the average bond length of each site, by determining the contribution of $\text{Fe}^{3+}\text{-O}$ bonds and Zn-O bonds to produce the average bond length. The ideal $\text{Fe}^{3+}\text{-O}$ (2.0155 Å) and Zn-O (2.1105 Å) bond lengths used for the averaging were calculated from the bond valence parameters of Brown & Altermatt (1985). These bond lengths give Fe^{3+}O_6 and ZnO_6 octahedra valence sums of exactly 3 and 2, respectively. Several refinement cycles were required before convergence of bond lengths and site occupancies were reached. These calculations showed a clear Zn-dominant site and a clear Fe-dominant site in both zemannites. This method was preferred instead of refining the occupancies with free variables because the free variable method resulted in a $\text{Fe}_{1.34}\text{Zn}_{0.66}$ composition for zemtype, inconsistent with both the EMPA data and the average bond length of the site, as calculated above. While such an issue was not encountered with zemmoc, for consistency the bond length method was used for both of the zemannites.

Hydrogen atoms were not visible in zemtype. The largest Q peaks were crystallographic ripples near to Te, and not

surrounding the channel oxygens. In zemmoc, although Q peaks were also visible around the Te atoms, hydrogen atoms were clearly visible around the channel oxygens. The H atom sites were refined at a constrained 0.90(5) Å from the oxygen atoms, with a thermal parameter 1.2 times greater than that of the associated oxygen atom. This represents the first time that hydrogen atom sites have been refined in zemannite. A representation of the H-bonding network is shown in Fig. 4. Half of the hydrogen atoms point towards the framework oxygen atoms, while the other half orientate themselves towards neighbouring channel water oxygen atoms. H3 is too close to a neighbouring oxygen (OW1), indicating that the half-occupied OW1 site must be vacant when this occurs. Miletich (1995a) also postulated a H-bonding network with half of the hydrogens pointing towards framework oxygen atoms and the other half towards other channel water oxygen atoms. Cametti *et al.* (2017) described a slightly different H-bonding network calculated from *ab initio* simulations. This calculated network has a strong H-bond from each of the two hexaaqua Mg^{2+} oxygen positions to different framework oxygen atoms, and one strong bond to an interstitial water molecule, however in this study the crystal-structure refinement shows no interstitial water. Therefore H-bonding environments in zemannite will be subtly different depending on the amount of interstitial water present in the channel.

The Mg valence in both zemannites is also greater than 15% above the expected value of 2, suggesting that the channels of zemannite force the channel oxygens slightly closer to the Mg atoms than in ideal Mg octahedra.

A full summary of bonding is shown in Table 3. A summary of bond valence is found in Tables 4 and 5 for zemtype and zemmoc, respectively, using the parameters of Brown & Altermatt (1985) for Mg, Fe and Zn, Brown (2002) for H and Mills & Christy (2013) for Te. Atomic coordinates, site occupancies and thermal parameters are shown in Tables 6 for zemtype and Tables 7 for zemmoc.

Table 3. Bond lengths (Å) comparison table for the two zemannites. *Mean value of Te–O bond length with primary bond lengths only is indicated with O'.

Zemtype		Zemmoc		
Te–O2	1.842(15)	Te–O2	1.858(12)	
Te–O1	1.893(4)	Te–O1	1.893(3)	
Te–O3	1.912(15)	Te–O3	1.895(9)	
Te–O2	2.882(16)	Te–O2	2.906(12)	
Te–O3	2.953(16)	Te–O3	2.909(10)	
Te–O3	3.157(12)	Te–O3	3.217(8)	
Te–O2	3.264(13)	Te–O2	3.238(8)	
<Te–O'>	1.882	<Te–O'>	1.882	
<Te–O>	2.557	<Te–O>	2.559	
M1–O3 (×3)	2.009(13)	M1–O3 (×3)	2.009(9)	
M1–O1 (×3)	2.177(13)	M1–O1 (×3)	2.165(8)	
<M1–O>	2.093	<M1–O>	2.087	
M2–O2 (×3)	1.972(14)	M2–O2 (×3)	1.986(10)	
M2–O1 (×3)	2.090(12)	M2–O1	2.109(8)	
<M2–O>	2.031	<M2–O>	2.048	
Mg–OW1 (×3)	2.026(19)	Mg–OW1 (×3)	2.031(14)	
Mg–OW2 (×3)	2.06(2)	Mg–OW2 (×3)	2.045(12)	
<Mg–O>	2.043	<Mg–O>	2.038	
H-bonding in zemmoc				
Donor O	d(D...H) (Å)	d(H...A) (Å)	d(D...A) (Å)	Acceptor O
OW1–H1	0.92(7)	2.06	2.69	O1
OW1–H2	0.94(7)	1.79	2.69	O1
<OW1–H>	0.93			
OW2–H3	0.901(15)	–	–	–
OW2–H4	1.00(7)	{ 2.00 2.33	{ 2.95 2.87	{ OW1 OW2
<OW2–H>	0.95			

*M1 is the Zn dominant site and M2 the Fe dominant site.

4.4. Choice of space group

Zemannite is a hexagonal mineral, but whether the type specimen crystallises in a non-centrosymmetric ($P6_3$) or centrosymmetric ($P6_3/m$) space group has never been determined beyond doubt using the type specimen. Miletich (1995a) presented evidence for a reduced symmetry model, $P6_3$, without using the type specimen. Cametti *et al.* (2017) also used the non-centrosymmetric space group, but were not able to refine the occupancies of each individual framework metal site due to the “the pseudo-symmetry imposed by the framework topology”. Our results corroborate the evidence for a reduced symmetry model and show that natural zemannite almost certainly crystallises in the space group $P6_3$. Refinements in both centrosymmetric and non-centrosymmetric space groups have been undertaken and analysed to determine the behaviour of zemannite crystals. The refinement in the centrosymmetric $P6_3/m$ group for zemtype showed almost no difference in the R -indices (0.0334 for 966 reflections with $F^2 > 2\sigma(F^2)$, compared with 0.0346 in $P6_3$). The refinement in $P6_3/m$ for zemmoc, however, showed a significant increase in R -indices (0.0300 for 569 reflections with $F^2 > 2\sigma(F^2)$, compared with 0.0254 in $P6_3$), which showed that the higher symmetry space group did not describe the structure as accurately as the non-centrosymmetric. The bond lengths for the two sites

are different in $P6_3$, with dominance of shorter Fe^{3+} –O bond lengths in one site (bond valence sum of 2.913 in the Fe^{3+} dominant site for zemtype, and 2.789 for zemmoc) and dominance of longer Zn–O bond lengths in the other (2.151 for zemtype, 2.179 in zemmoc), indicative of ordering of the two cations.

4.5. Comparison of the two zemannite crystals

Zemtype and zemmoc do not display significant differences in their unit cells, which have parameters within 0.02 Å of each other.

The average Te^{4+} –O bond lengths for the two zemannites are similar, despite the varying chemical compositions. Te^{4+} forms triangular pyramids in zemannite, with three primary bonds to oxygen atoms. Both zemannites display an average primary Te^{4+} –O length of 1.882 Å. These lengths are comparable to the 1.911 ± 0.077 Å expected for short Te^{4+} –O bonds (Mills & Christy, 2013). Bond valence sums for Te^{4+} are 3.933 *vu* for zemtype and 3.926 *vu* for zemmoc after the inclusion of four secondary bonds, resulting in TeO_7 polyhedra (Fig. 5). Unlike some Te^{4+} polyhedra, which display significant irregularity in their geometry, the TeO_7 unit in zemannite is relatively symmetrical (Christy & Mills, 2013). The secondary bonds increase the overall stability of the framework by providing two cross-links to both the O2 and O3 sites, further linking each Te centre to its neighbouring three M_2O_9 dimers (Fig. 6).

The octahedral sites have M –O bond lengths split into two groups of three near-identical bond lengths, in which the two lengths are separated by a distance greater than 0.1 Å. The site dominance can be distinguished by the average bond lengths, which are shorter for the Fe^{3+} dominant site. The Zn-dominant site has an average M –O bond length of 2.093 Å in zemtype and 2.087 Å in zemmoc, while the Fe-dominant site has an average bond length of 2.031 Å in zemtype and 2.048 Å in zemmoc.

Average Mg–O bond lengths were calculated to be 2.043 Å in zemtype and 2.038 Å in zemmoc for the hexaqua magnesium cation, $[\text{Mg}(\text{H}_2\text{O})_6]^{2+}$. These cations and the atoms in associated water molecules have an ideal occupancy of 0.5 in natural zemannites, though in both crystal structures studied the occupancy was refined to slightly greater than 0.5. The bond valence sum for Mg is rather high, due to the channel oxygen atoms being forced to sit slightly closer to Mg than is ideal by the constraints of the channel. It is also possible that a small fraction of the Fe and Mn are bivalent and substitute for the Mg in the channel metal site.

4.6. Degree of hydration

The degree of hydration calculated from the crystal structures of both natural and synthetic zemannites is slightly greater than 3 H_2O molecules *pfu* of zemannite, which is lower than the 4.5 *pfu* specified by Miletich (1995a) and 3.9 by Cametti *et al.* (2017). The remaining 1.5 water molecules are reported by Miletich (1995a) as corresponding to interstitial water molecules unattached to

Table 4. Bond valence sums (in valence units, νu) for zemtype*.

Atom	Te	M1	M2	Mg	Σ
O1	1.179	0.278 ($\times 3 \downarrow$)	0.409 ($\times 3 \downarrow$)		1.866
O2	1.335, 0.106, 0.042		0.562 ($\times 3 \downarrow$)		2.045
O3	1.128, 0.089, 0.054	0.439 ($\times 3 \downarrow$)			1.710
OW1				0.407 ($\times 3 \downarrow$)	0.407
OW2				0.371 ($\times 3 \downarrow$)	0.371
Σ	3.933	2.151	2.913	2.332	

Table 5. Bond valence sums (in valence units, νu) for zemmoc*.

Atom	Te	M1	M2	Mg	H1	H2	H3	H4	Σ
O1	1.179	0.288 ($\times 3 \downarrow$)	0.388 ($\times 3 \downarrow$)		0.162 ($\times 0.5 \rightarrow$)	0.258 ($\times 0.5 \rightarrow$)			2.065
O2	1.284, 0.100, 0.044		0.541 ($\times 3 \downarrow$)						1.969
O3	1.173, 0.099, 0.047	0.439 ($\times 3 \downarrow$)							1.757
OW1				0.401 ($\times 3 \downarrow$)	0.955	0.889		(\rightarrow -) 0.182	2.063
OW2				0.386 ($\times 3 \downarrow$)			1.022	0.717, (\rightarrow -) 0.103	2.022
Σ	3.926	2.179	2.789	2.362	1.117	1.147	1.022	1.003	

*M1 is the Zn dominant site and M2 the Fe dominant site. M1 bond valence is thus calculated using Zn parameters and M2 using Fe(III) parameters, reflective of the dominant cation in the sites.

Table 6. Fractional atomic coordinates, occupancies and atomic displacement parameters for the atomic sites of zemtype.

Atom	x	y	z	Occ	U_{eq}	U_{11}	U_{22}	U_{33}	U_{23}	U_{13}	U_{12}
Te1	0.45432(4)	0.49496(4)	0.4824(7)	1	0.01099(12)	0.01163(18)	0.01108(18)	0.01211(18)	-0.0001(6)	0.0002(7)	0.00707(13)
Zn1	2/3	1/3	0.6739(2)	0.7844	0.0143(9)	0.0161(13)	0.0161(13)	0.0105(19)	0	0	0.0081(6)
Fe1	2/3	1/3	0.6739(2)	0.2156	0.0143(9)	0.0161(13)	0.0161(13)	0.0105(19)	0	0	0.0081(6)
Zn2	2/3	1/3	0.2930(2)	0.1793	0.0075(8)	0.0072(11)	0.0072(11)	0.0080(19)	0	0	0.0036(6)
Fe2	2/3	1/3	0.2930(2)	0.8207	0.0075(8)	0.0072(11)	0.0072(11)	0.0080(19)	0	0	0.0036(6)
O1	0.6553(5)	0.4938(5)	0.475(2)	1	0.0110(10)	0.0136(18)	0.0122(18)	0.010(3)	0.003(4)	0.004(5)	0.0084(15)
O2	0.5015(16)	0.6424(15)	0.663(2)	1	0.018(3)	0.027(6)	0.010(4)	0.011(4)	-0.004(3)	0.005(4)	0.005(3)
O3	0.5151(14)	0.6602(16)	0.306(2)	1	0.015(2)	0.007(3)	0.018(5)	0.022(6)	0.005(4)	-0.001(3)	0.007(3)
Mg1	1	1	0.557(2)	0.50(2)	0.038(4)	0.037(5)	0.037(5)	0.040(8)	0	0	0.019(3)
OW1	1.192(2)	1.071(2)	0.391(2)	0.50(2)	0.038(5)						
OW2	1.122(3)	1.198(2)	0.724(3)	0.50(2)	0.050(6)						

Table 7. Fractional atomic coordinates, occupancies and atomic displacement parameters for the atomic sites of zemmoc.

Atom	x	y	z	Occ	U_{eq}	U_{11}	U_{22}	U_{33}	U_{23}	U_{13}	U_{12}
Te1	0.45648(3)	0.49692(3)	0.4845(4)	1	0.00992(19)	0.0096(2)	0.0091(2)	0.0123(3)	-0.0006(3)	-0.0002(3)	0.00550(13)
Zn1	2/3	1/3	0.6734(2)	0.7528	0.0123(5)	0.0120(7)	0.0120(7)	0.0128(12)	0	0	0.0060(4)
Fe1	2/3	1/3	0.6734(2)	0.2472	0.0123(5)	0.0120(7)	0.0120(7)	0.0128(12)	0	0	0.0060(4)
Zn2	2/3	1/3	0.29295(14)	0.3371	0.0076(5)	0.0070(7)	0.0070(7)	0.0087(13)	0	0	0.0035(3)
Fe2	2/3	1/3	0.29295(14)	0.6629	0.0076(5)	0.0070(7)	0.0070(7)	0.0087(13)	0	0	0.0035(3)
O1	0.6572(4)	0.4955(4)	0.4778(14)	1	0.0105(8)	0.0095(15)	0.0114(15)	0.012(2)	0.007(3)	0.007(3)	0.0061(12)
O2	0.5074(9)	0.6491(10)	0.6635(18)	1	0.0182(16)	0.017(4)	0.016(4)	0.030(4)	-0.003(3)	-0.001(3)	0.014(3)
O3	0.5130(9)	0.6551(8)	0.3040(13)	1	0.0129(14)	0.014(3)	0.010(3)	0.004(3)	0.005(3)	-0.001(2)	-0.002(2)
Mg1	1	1	0.5590(13)	0.56(2)	0.018(2)	0.013(3)	0.013(3)	0.029(4)	0	0	0.0064(13)
OW1	1.1910(15)	1.0629(15)	0.3922(17)	0.56(2)	0.025(3)						
H1	1.281(16)	1.150(18)	0.44(3)	0.56(2)	0.030						
H2	1.290(15)	1.09(2)	0.45(3)	0.56(2)	0.030						
OW2	1.1334(13)	1.2003(13)	0.7157(15)	0.56(2)	0.025(3)						
H3	1.14(3)	1.19(3)	0.832(7)	0.56(2)	0.030						
H4	1.039(19)	1.17(2)	0.63(2)	0.56(2)	0.030						

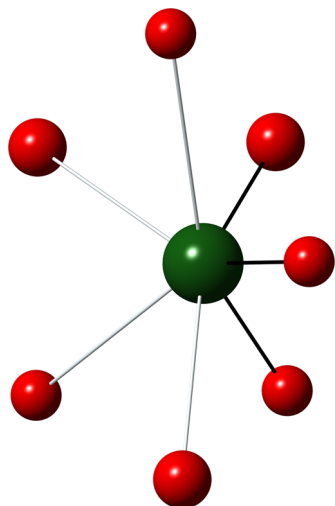


Fig. 5. The Te^{4+}O_7 unit in zemannite. The Te atom is in dark green and the oxygen atoms in red. The three primary bonds forming the trigonal pyramidal arrangement are marked in black and are on the right hand side of the diagram. The longer secondary bonds are in grey.

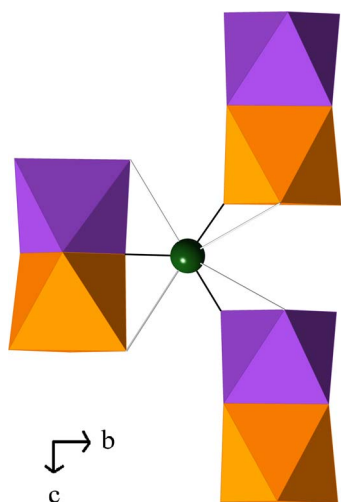


Fig. 6. The bridging role of the longer $\text{Te}^{4+}\text{-O}$ bonds in zemannite. Two secondary bonds are formed to the dimer hosting O1 in the Te-O1 bond and one secondary bond is formed to each of the two other neighbouring dimers.

the channel Mg cations. Three H_2O molecules *pfu* are reported in synthetic zemannite isomorphs with the formulae $\text{Na}_2[\text{M}_2^{2+}(\text{Te}^{4+}\text{O}_3)_3]\cdot 3\text{H}_2\text{O}$, for $\text{M} = \text{Zn}$ or Co (Miletich, 1995b). Na in these two zemannite-like structures is not found on a special position (unlike in natural zemannites, in which Mg occupies the centre of the hexagonal channels, which is a special position with coordinates 1,1,*z*). Na–O bonds are also longer on average than Mg–O, leaving less remaining space for interstitial water. It is not essential for Na in zemannite to be found away from the centre of the channels. The authors have recently synthesised a Na–Zn– Fe^{3+} zemannite that contains Na in the centre of the channels

on the same special position occupied by Mg in type zemannite.

Despite these observations on Na zemannites, the lack of any obvious crystallographic evidence for interstitial water is puzzling, as this is reported by both Miletich (1995a) and Cametti *et al.* (2017) for natural zemannite samples from Moctezuma. The largest residual peaks in the Fourier maps for the two zemannites studied were all little more than $2e^- \text{ \AA}^{-3}$, and none of these peaks stably refined as oxygen atoms in channel sites when added into the structure. Both zemannites appears to contain slightly more than 3 H_2O molecules *pfu*, an artefact of the occupancy of the channel atoms increasing above 0.5, but there is little evidence for interstitial water. Analysis of type zemannite in this study has shown that it does not contain extra interstitial water molecules. Nonetheless, the extra hydration observed in these studies is not unexpected due to the zeolitic nature of zemannite, and is reflected in the proposed formula change for zemannite below.

For these reasons the end-member formula of zemannite should be revised to $\text{Mg}_{0.5}\text{ZnFe}^{3+}(\text{Te}^{4+}\text{O}_3)_3\cdot(3+n)\text{H}_2\text{O}$, where $0 \leq n \leq 1.5$, from $\text{Mg}_{0.5}\text{ZnFe}^{3+}(\text{Te}^{4+}\text{O}_3)_3\cdot 4.5\text{H}_2\text{O}$.

5. Conclusions and future zemannite work

Natural zemannite has been definitively shown to have Mg dominant over Na within the channels of the zeolitic hexagonal framework of this mineral (Na <0.05 ppm in zemannite). In addition, natural zemannite crystals have been shown to refine in the non-centrosymmetric space group, $P6_3$, allowing for clear ordering between the Fe^{3+} and Zn sites. More zemannite-type minerals may be present in nature, incorporating different cations, either in the framework or in the channels. Further zemannite analogues might have been overlooked due to their similarity to type zemannite. Na, K or even Ca analogues of zemannite, in which these elements substitute for Mg in the hexagonal channels, would have a near-identical appearance to zemannite. Na analogues of zemannite have readily been synthesised, with two currently published structures (Miletich, 1995b) and one structure recently synthesised by the authors, but not yet found in nature. The elemental differences would not be discernible without performing microprobe analyses. There are cases in which a relatively rare mineral, with an appearance similar to a more common one, has been overlooked for many years (*e.g.* Mills *et al.*, 2010). Hazen *et al.* (2015) recently suggested that a large number of new Na minerals are believed to exist and have been overlooked by scientists, mostly because they are typically colourless or have a similar appearance to other known or well-known phases.

Zemannite-like selenites are also yet to be found in nature. The relative prevalence of natural tellurite-based zemannites (compared to other secondary tellurium minerals) and the previous synthesis of zemannite-like selenites (Wildner, 1993) suggests that a selenite analogue(s) may exist in nature. The relationship between selenium and tellurium analogues has been explored in the chalcocite-type structures (*e.g.* Rumsey *et al.*, 2017; Charykova *et al.*, 2017).

Localities rich in secondary selenium mineralogy such as the El Dragón Mine, Antonio Quijarro Province, Potosí Department, Bolivia (19°49'S, 65°55'W) should be further examined for signs of hexagonal prismatic minerals (e.g. Grundmann & Förster, 2017).

We make the following recommendations based on this study and for future study of zemannite-type minerals:

1. $P6_3$ (non-centrosymmetric) symmetry should always be tested for natural zemannite-like structures. If it is possible to refine in this space group and also refine the occupancies of the octahedral metal sites, this provides information which is otherwise obscured by the bond lengths of the cations being averaged out.
2. Due to Na and Zn peak overlaps, it is most rigorous to test for the presence of Na in zemannites using a technique such as ICP-AES to back up the microprobe data. In this case for instance, Na needs to be above 1200 ppm before it can be considered to be above background, whereas for ICP-AES Na only needs to be above 0.05 ppm (3σ).
3. We recommend that the formula of zemannite be revised to $Mg_{0.5}ZnFe^{3+}(Te^{4+}O_3)_3 \cdot (3+n)H_2O$, where $0 \leq n \leq 1.5$, from the currently accepted $Mg_{0.5}ZnFe^{3+}(Te^{4+}O_3)_3 \cdot 4.5H_2O$, to better reflect the variable degree of hydration. Type zemannite has $n = 0.06$, prompting this change, as the currently accepted formula is not accurate for type zemannite.

Acknowledgements: This study has been partly funded by The Ian Potter Foundation grant “tracking tellurium” to SJM, and a Museums Victoria 1854 Student Scholarship awarded to OPM, which we gratefully acknowledge. Microprobe work was funded through Natural Environment Research Council grant NE/M010848/1 “Tellurium and Selenium Cycling and Supply” to Chris J. Stanley, which we also gratefully acknowledge.

We thank Kim Tait (Royal Ontario Museum, Toronto) for loan and access to the zemannite type specimen, without which this study would not have been possible. We thank David Paul (Museums Victoria) for his assistance in photographing the type zemannite crystal and Simon Hinkley (Museums Victoria) for assistance in photographing the zemmoc specimen (M53996).

This research was undertaken in part using the MX2 beamline at the Australian Synchrotron, part of ANSTO, and made use of the Australian Cancer Research Foundation (ACRF) detector.

We thank Timothy Hudson (University of Melbourne) for his help with the single crystal data collection on zemtype, Christopher Kingsbury (University of Melbourne) for his assistance in refining the structures, Augustine Doronila (University of Melbourne) for his assistance with ICP-AES analysis of zemmoc, and Igor Pekov (Moscow State University) and Brendan Abrahams (University of Melbourne) for their insightful comments. We also thank Editor-in-Chief Sergey Krivovichev and two anonymous reviewers for their comments, which significantly improved the manuscript.

References

- Brown, I.D. (2002): The chemical bond in inorganic chemistry. Oxford University Press.
- Brown, I.D. & Altermatt, D. (1985): Bond-valence parameters obtained from a systematic analysis of the inorganic crystal structure database. *Acta Cryst. B*, **41**, 244–247.
- Bruker (2001): SADABS and XPREP. Bruker AXS Inc, Madison, WI, USA.
- Cametti, G., Churakov, S., Armbruster, T. (2017): Reinvestigation of the zemannite structure and its dehydration behavior: a single-crystal X-ray and atomistic simulation study. *Eur. J. Mineral.*, **29**, 53–61.
- Charykova, M.V., Lelet, M.I., Krivovichev, V.G., Ivanova, N.M., Suleimanov, E.V. (2017): A calorimetric and thermodynamic investigation of the synthetic analogue of chalcocite, $CuSeO_3 \cdot 2H_2O$. *Eur. J. Mineral.*, **29**, 269–277.
- Christy, A. & Mills, S. (2013): Effect of lone-pair stereoactivity on polyhedral volume and structural flexibility: application to $Te^{IV}O_6$ octahedra. *Acta Cryst. B*, **69**, 446–456.
- Christy, A.G., Mills, S.J., Kampf, A.R. (2016): A review of the structural architecture of tellurium oxycompounds. *Mineral. Mag.*, **80**, 415–454.
- Grundmann, G. & Förster, H. (2017): Origin of the El Dragón selenium mineralization, Quijarro province, Potosí, Bolivia. *Minerals*, **7**, 68.
- Hazen, R.M., Hystad, G., Downs, R.T., Golden, J.J., Pires, A.J., Grew, E.S. (2015): Earth’s “missing” minerals. *Am. Mineral.*, **100**, 2344–2347.
- Kabsch, W. (2010): XDS. *Acta Cryst. D*, **66**, 125–132.
- Mandarino, J.A. & Williams, S.J. (1961): Five new minerals from Moctezuma, Sonora, Mexico. *Science*, **133**, 2017.
- Matzat, E. (1967): Die Kristallstruktur eines unbenannten zeolithartigen Tellurminerals, $\{(Zn,Fe)_2[TeO_3]_3\}Na_x H_{2-x}yH_2O$. *Tschermaks Miner. Petrogr. Mitt.*, **12**, 108–117.
- Miletich, R. (1995a): Crystal chemistry of the microporous tellurite minerals zemannite and kinichilite, $Mg_{0.5}[Me^{2+}Fe^{3+}(TeO_3)_3] \cdot 4.5H_2O$, ($Me^{2+}=Zn;Mn$). *Eur. J. Mineral.*, **7**, 509–523.
- (1995b): The synthetic microporous tellurites $Na_2[Me_2(TeO_3)_3] \cdot 3H_2O$ ($Me = Zn, Co$): crystal structure, de- and rehydration, and ion exchange properties. *Monatsh. Chem.*, **126**, 417–430.
- Mills, S.J. & Christy, A.G. (2013): Revised values of the bond-valence parameters for $Te^{IV}-O$, $Te^{VI}-O$ and $Te^{IV}-Cl$. *Acta Cryst. B*, **69**, 145–149.
- Mills, S.J., Kampf, A.R., Poirier, G., Raudsepp, M., Steele, I.M. (2010): Auriacusite, $Fe^{3+}Cu^{2+}AsO_4O$, the first M^{3+} member of the olivenite group, from the Black Pine mine, Montana, USA. *Mineral. Petrol.*, **99**, 113–120.
- Pasero, M. (2018): *The New IMA List of Minerals*, <http://nrmima.nrm.se/>.
- Rumsey, M.S., Welch, M.D., Mo, F., Kleppe, A.K., Spratt, J., Kampf, A.R., Raanes, M.P. (2017): Millsite $CuTeO_3 \cdot 2H_2O$: a new polymorph of teinite from Gråurdfjellet, Oppdal kommune, Norway. *Mineral. Mag.*, **82**, 433–444.
- Sheldrick, G.M. (2008): A short history of SHELX. *Acta Cryst. A*, **64**, 112–122.
- (2015): Crystal structure refinement with SHELXL. *Acta Cryst. C*, **71**, 3–8.
- Wildner, M. (1993): Zemannite-type Selenites: Crystal structures of $K_2[Co_2(SeO_3)_3] \cdot 2H_2O$ and $K_2[Ni_2(SeO_3)_3] \cdot 2H_2O$. *Mineral. Petrol.*, **48**, 215–225.

Received 19 April 2018

Modified version received 21 June 2018

Accepted 31 July 2018